Imaging B cells in a mouse model of multiple sclerosis using ^{64}Cu-Rituximab-PET

Michelle L. James[1,2], Aileen Hoehne[1], Aaron T. Mayer[1], Kendra Lechtenberg[2], Monica Moreno[2], Gayatri Gowrishankar[1], Ohad Ilovich[1], Arutselvan Natarajan[1], Emily M. Johnson[1,2], Joujou Nguyen[1], Lisa Quach[2], May Han[2], Marion Buckwalter[2], Sudeep Chandra[3], Sanjiv S. Gambhir[1]*.

Affiliations:

[1]*Department of Radiology, Stanford University, Stanford CA, 943065, USA*

[2]*Department of Neurology and Neurological Sciences, Stanford University, Stanford CA, 943065, USA*

[3]*Department of Translational Medicine, Clinical and Translational Imaging, Novartis Institute of Biomedical Research, Cambridge, MA, USA.*

*Corresponding Author: Sanjiv Gambhir, 318 Campus Dr, E150, Stanford, CA 94305, USA. V: (650)725-6175; F: (650)723-8649 (sgambhir@stanford.edu).

First Author: Michelle James, 3165 Porter Drive, Stanford, CA 94304. V: (650)721-3324; F: (650)724-4948 (mljames@stanford.edu).

Running title: Imaging B cells in EAE mice using PET

Word count: 4999

ABSTRACT

B lymphocytes are a key pathological feature of multiple sclerosis (MS), and are becoming an important therapeutic target for this condition. Currently, there is no approved technique to non-invasively visualize B cells in the central nervous system (CNS) to monitor MS disease progression and response to therapies. Here we evaluated ^{64}Cu-Rituximab, a radiolabeled antibody specifically targeting the human B cell marker CD20, for its ability to image B cells in a mouse model of MS using positron emission tomography (PET). **Methods:** To model CNS infiltration by B cells, experimental autoimmune encephalomyelitis (EAE) was induced in transgenic mice that express human CD20 on B cells. EAE mice were given subcutaneous injections of Myelin Oligodendrocyte Glycoprotein fragment$_{1\text{-}125}$ (MOG$_{1–125}$) emulsified in complete Freund's adjuvant. Control mice received complete Freund's adjuvant alone. PET imaging of EAE and control mice was performed 1, 4, and 19h following ^{64}Cu-Rituximab administration. Mice were perfused and sacrificed after final PET scan, and radioactivity in dissected tissues was measured with a gamma-counter. CNS tissues from these mice were immunostained to quantify B cells or further analyzed via digital autoradiography. **Results:** Lumbar spinal cord PET signal was significantly higher in EAE mice compared to controls at all evaluated time points (e.g., 1h post-injection: 5.44 ± 0.37 vs. 3.33 ± 0.20 %ID/g, $p<0.05$). ^{64}Cu-Rituximab-PET signal in brain regions ranged between 1.74 ± 0.11 and 2.93 ± 0.15 %ID/g for EAE mice compared to

2

1.25±0.08 and 2.24±0.11%ID/g for controls, $p<0.05$ for all regions except striatum and thalamus at 1h post-injection. Similarly, *ex vivo* biodistribution results revealed notably higher ^{64}Cu-Rituximab uptake in brain and spinal cord of huCD20tg EAE, and B220 immunostaining verified that increased ^{64}Cu-Rituximab uptake in CNS tissues corresponded with elevated B cells.

Conclusion: B cells can be detected in the CNS of EAE mice using ^{64}Cu-Rituximab-PET. Results from these studies warrant further investigation of ^{64}Cu-Rituximab in EAE models and consideration of use in MS patients to evaluate its potential for detecting and monitoring B cells in the progression and treatment of this disease. These results represent an initial step toward generating a platform to evaluate B cell-targeted therapeutics en route to the clinic.

Key words: Multiple sclerosis, EAE, B cells, Rituximab, PET.

INTRODUCTION

There is a growing appreciation of the importance of B cells in MS (*1*). MS patients exhibit B cells in brain parenchyma, meninges, and in primary and secondary lymphoid tissue. In meninges, B cells are reported in ectopic lymphoid follicle like structures (FLS) (*2*). FLS vary in the number of structures per case and in cells per structure, from 50 to several hundreds to thousands of B cells. These structures have been implicated in maintaining autoimmunity and exacerbating disease. Antibodies targeting CD20 expressed on both immature and mature B cells have exhibited impressive clinical results. In phase two/three trials of Rituximab (Rituxan, Genentech and BiogenIdec, RTX), treatment was associated with a significant reduction in the number of relapses and decreased lesion formation in a subgroup of patients (*3*). Rituximab's successors, Ocrelizumab (Roche, Genentech) and Ofatumumab (Novartis), have since shown improved biologic properties and reduced immunogenicity (*4*). While CD20 antibody therapy is clearly beneficial to MS patients, no clinical tool exists to evaluate whether there is a preferential benefit in patients with B-cell driven disease.

A landmark study utilizing patient postmortem tissue and standard immunohistochemistry techniques identified four primary lesion types in MS, with Type II patients having the largest involvement of B cell subsets and best

likelihood of response to plasma exchange therapy (*5*). PET imaging may aid in identifying living patients most likely to respond to B cell targeted therapies (i.e., patient stratification). Radiological imaging has the advantage of being non-invasive and dynamic, allowing clinicians to monitor response longitudinally without the need for invasive biopsies. Furthermore, biopsies are not always possible in MS patients and they do not capture global information from all lesions. PET imaging could provide clues regarding the extent and size of B cell FLS in the CNS, the degree of peripheral vs. central B cell involvement, and the respective longitudinal changes over the course of disease or treatment. To the best of our knowledge, PET imaging of B cells in MS has not yet been studied. For these reasons, there exists a compelling need for the development and application of a B cell specific PET tracer for monitoring MS.

Here we propose the application of an anti-CD20 immunoPET tracer, ^{64}Cu-Rituximab, for imaging B cells in EAE mice, a rodent model used to study MS. We will test our hypothesis that B cells can be detected systemically and in the CNS of living mice displaying MS disease characteristics. These experiments will provide critical insights that will help guide future clinical studies to evaluate ^{64}Cu-Rituximab-PET for its potential to stratify patients, predict responders, and improve clinical decision making for patients with MS and other B cell related autoimmune diseases.

MATERIALS AND METHODS

Study Design

Experiments involving animals were performed using protocols approved by Stanford University's Institutional Animal Care and Use Committee. Three groups of huCD20Tg mice (*6*), expressing human CD20 on all B cells, were used for these studies. The first group was for histological analysis of B cell numbers after induction of EAE ($n = 7$) versus naive ($n = 5$) mice (sans Rituximab), the second group was for flow cytometry of B cells in spleen and blood samples 19 hours after intravenous treatment with non-radioactive Rituximab (1 or 3 μg in 150 μL 0.9% sodium chloride solution, $n = 5$ and $n = 4$ respectively) or vehicle (0.9% sodium chloride solution, $n = 6$), and the third group was for *in vivo* PET studies ($n = 4$ per group), *ex vivo* biodistribution ($n = 5$ per group), *ex vivo* autoradiography ($n = 3$ per group), and histology ($n = 4$ per group). PET imaging time points of 1, 4, and 19 hours were chosen (along with *ex vivo* biodistribution at 24 hours) since our group has observed suitable signal-to-background with ^{64}Cu-Rituximab in huCD20tg mice at 4 and 24 hours after tracer injection. Previously we have shown that signal in spleen (organ containing a large pool of CD20-expressing B cells) decreases at 48 hours compared to the high-to-background signal observed at 4 and 24 hours (*7*). To assess the specificity of ^{64}Cu-Rituximab for imaging human CD20 in EAE mice, control C57BL/6 mice

devoid of human CD20 were induced with EAE (n = 3) and imaged with ^{64}Cu-Rituximab, with the goal of comparing the PET signal in these mice with that of naive C57BL/6 mice (n = 3) and huCD20tg EAE mice (containing human CD20, n = 4). huCD20Tg and littermate control mice were backcrossed to the C57BL/6 genetic background for >12 generations for these studies. [64]Cu was chosen for these initial studies due to previous experience (*7*) and access to an approved institutional investigational new drug application for ^{64}Cu-Rituximab. Such studies can also be performed with [89]Zr-labeled Rituximab (e.g., clinical imaging of lymphoma) (*8*).

EAE Induction

Mice (4-6 months old) were immunized subcutaneously with a total of 200 μg of MOG_{1-125} protein emulsified in complete Freund's adjuvant containing 5 mg/ml of mycobacteria (customized kit from Hooke Laboratories Inc., MA). Mice received an intravenous injection of 200 ng pertussis toxin (Hooke Laboratories Inc.) at the time of immunization and 48 h later. Mice were weighed and examined daily for clinical signs of EAE using standard scoring – i.e., 0, no paralysis; 1, loss of tail tone; 2, hind limb weakness or paresis; 3, hind limb paralysis; 4, hind limb paralysis and forelimb paresis; 5-moribund or deceased.

Immunostaining and Quantitation

Brains and spinal cords were fixed in 4% paraformaldehyde in phosphate buffer for 24 hours then sunk in 30% sucrose in phosphate buffered saline. Free-floating 40 μm sagittal sections were collected through the entire brain, and 40 μm transverse sections were collected through the lumbar and thoracic/cervical spinal cord using Microm HM 450 sliding microtome (Thermo Scientific) and stored in cryoprotective medium at -20°C. Immunostaining was performed following standard protocols and utilized the following antibodies: biotinylated anti-B220/CD45R (1:500, BD Pharmigen). For visualization, sections were immersed in Vectastain Elite ABC kit (Vector Laboratories) followed by 0.05% 3,3-diaminobenzidine (Sigma) in TBS with 0.03% H_2O_2. For image acquisition of B220-labelled B cells, digitized images were captured with Zeiss AxioImager M2 light microscope using AxioVision software. B cells were quantified by a blinded experimenter on an Olympus upright light microscope at 40X magnification in 3 whole sagittal brain sections per mouse and in 5 whole spinal cord sections per mouse. B cell densities were calculated using brain or spinal cord section areas which were measured using ImageJ software.

Fluorescence-activated cell sorting (FACS)

Mice were anesthetized with isoflurane in an induction chamber. The submandibular vein was punctured with a 25-gauge needle and 4-6 drops of blood were collected and placed in a collection tube containing 10% heparin. Blood samples were added to 4 mL of 1X Lysis buffer (Biolegend) and left at RT for 10 minutes followed by incubation at 37 °C for 5 minutes with shaking. Cells were washed twice with sterile 1X PBS and spun at 350 x g for 5 minutes. Pellets were resuspended in FACS buffer with 1% bovine serum albumin for subsequent flow cytometric analysis.

Spleens were harvested and minced in 10mm tissue culture plates containing sterile 1X PBS (without calcium chloride and magnesium chloride) then twice filtered through a 70 µm cell strainer (BD 352350) to achieve a single cell suspension. The cells were pelleted by centrifugation (350 x g) and the pellet was resuspended in 5 mL of 1X Lysis Buffer and incubated on ice for 5 minutes with occasional shaking. The reaction was stopped by diluting the Lysis Buffer with 20-30 mL of 1X PBS. The cells were spun (350 x g) and the supernant was discarded. The pellet was washed and resuspended in FACS buffer with 1% bovine serum albumin for subsequent flow cytometric analysis.

Cells were immunostained immediately after blocking of Fc receptors with anti-CD16/32 (BD Biosciences) to prevent nonspecific binding. B lymphocytes were identified by allophycocyan (APC)-labeled anti-mouse CD19 (Biolegend 115512) and Fluorescein isothiocyanate (FITC)-labeled anti-mouse B220/CD45R (BioLegend 103205). A fixable dead cell stain (Molecular Probes L23101) was used to distinguish between live and dead cells.

DOTA Conjugation

Conjugation of rituximab with 1,4,7,10-tetraazacyclododecane-1,4,7,10-tetraacetic acid (DOTA) was performed using standard published procedures and metal-free buffers (9). The number of chelators coupled per antibody molecule was estimated to be 1.8 via MALDI-TOF MS by comparison of rituximab with DOTA-rituximab.

Radiosynthesis

Radiolabeling of DOTA-rituximab with ^{64}CuCl$_2$ (University of Wisconsin, Madison, WI, USA) was completed using standard methods and metal-free buffers (9). ^{64}Cu-Rituximab was obtained with high specific radioactivity (>75 GBq/μmol), radiochemical purity (>99%), and labeling efficiency (70-95%), and

formulated in phosphate-buffered saline (0.1 mol/L NaCl, 0.05 mol/L sodium phosphate, pH 7.4). Immunoreactivity of ^{64}Cu-DOTA-Rituximab was evaluated in quadruplicates using previously described procedures (*10*), with a 4:1 silicone oil–mineral oil mixture in place of the described phthalate oil mixture. Ramos CD20+ cells (3×10^5 to 3×10^6 cells) were used to determine the immunoreactive fraction – which was found to be >75%.

PET Imaging

PET images were acquired using a hybrid microPET/computed tomography (CT) scanner (Inveon, Siemens), and reconstructed using 2 iterations of 3-dimensional ordered subsets expectation maximization algorithm (12 subsets) and 18 iterations of the accelerated version of 3D-MAP (i.e., FASTMAP) – matrix size of 128 × 128 × 159. Attenuation correction was applied to dataset from CT image. No partial volume corrections were performed. Mice were anesthetized using isoflurane gas (2.0-3.0% for induction, 1.5-2.5% for maintenance). Each mouse was injected with ^{64}Cu-Rituximab (1.3-3.7 MBq) intravenously via tail vein. CT images were acquired just before each PET scan to provide an anatomic reference frame for the respective PET data. The calibration factor for ^{64}Cu PET was determined using a 20 mL syringe containing a known amount of radioactive ^{64}Cu. PET and CT image files were co-registered and analyzed with Inveon

Research Workspace software (IRW, version 4.0; Siemens) and VivoQuant image analysis software (version 2.0, inviCRO). IRW was used to generate images for figures, while VivoQuant was used to quantify tracer uptake in specific brain regions and spinal cord. For analysis of brain uptake, a 3-dimensional mouse brain atlas was fitted to PET/CT images and radioactivity concentrations were obtained using automated regions of interest (ROIs) for cerebellum, cortex, hippocampus, hypothalamus, medulla, midbrain, pons, striatum, and thalamus. For analysis of ^{64}Cu-Rituximab uptake in spinal cord, the vertebral column was first isolated by Otsu thresholding and the resulting ROI was made immutable. An ROI of the spinal cord was then drawn, from the caudal end of the skull to the pelvis, using the segmented vertebral column as a guide. For analysis of regional variations in spinal cord PET signal, the spinal cord was divided, using L1-L5 as landmarks, into cervical/thoracic and lumbar ROIs (Supplemental Figure 1A-C). Radioactive concentration (Bq/cc) for each ROI was obtained and subsequently divided by the decay corrected dose at the time of PET scan for each mouse and multiplied by 100 to determine the percentage of injected dose per gram (%ID/g).

Ex Vivo Biodistribution and Autoradiography

Tissues were collected for biodistribution and *ex vivo* autoradiography, 24 hours post-injection of ^{64}Cu-Rituximab, using previous methods (*11*).

Statistics

Statistical analyses were performed using GraphPad Prism (version 6). Data are expressed as mean ± standard error mean, unless otherwise indicated. Two-tailed Mann-Whitney U-tests were used for group comparisons, 2way analysis of variance (ANOVA) tests were used for multiple comparisons, and a p-value of 0.05 was considered significant.

RESULTS

EAE was induced in huCD20tg mice to evaluate the utility of ^{64}Cu-Rituximab as a PET tracer for imaging B cells in MS. huCD20tg mice were chosen for these studies, in lieu of C57BL/6 mice, since their B cells express the more clinically relevant PET target, human CD20. Monson et al. reported that the expression of human CD20 by B cells does not significantly affect the immune response leading to EAE, as determined by comparing peak disease severity between huCD20tg and wild-type littermates following EAE induction via subcutaneous immunization with MOG_{1-125} (*6*). The peak disease severity for mice in our studies was observed on day 14 – clinical scores ranged from 2.5-4.0. (Supplemental Fig. 2).

B220 immunostaining of brain and spinal cord at the peak of EAE disease severity (i.e., score 2.5-4.0) was conducted to first verify that B cells infiltrate the CNS of huCD20tg EAE mice and that this model can therefore be used for evaluation of ^{64}Cu-Rituximab. Immunohistochemistry results (Fig. 1) revealed significantly more B220 positive cells in EAE CNS tissues compared with age-matched naive mice (brain and meninges: 3.09 ± 0.63 vs. 0.62 ± 0.18 cells/mm^2, p=0.018; lumbar spinal cord: 28.57 ± 4.96 vs. 2.20 ± 0.49 cells/mm^2, p=0.003; thoracic/cervical spinal cord: 17.15 ± 4.35 vs. 1.86 ± 0.39 cells/mm^2, p=0.003). Of note, there were clusters of B cells in the meninges of EAE huCD20tg mice (Fig. 1A) similar to B cell FLS found in the meninges of patients with secondary progressive MS (*12*). B220 positive cells observed in spinal cord were more numerous than those found in brain overall (Fig. 1B), but were more diffusively distributed in the white matter of the cord, as opposed to existing in clusters.

Since Rituximab is known to potently deplete B cells even at low doses (*13,14*), we set out to investigate whether a typical PET tracer dose of Rituximab could lead to a pharmacological effect. The specific activity of ^{64}Cu-Rituximab routinely achieved was 1.3 MBq/µg, meaning that a typical PET tracer dose of 1.3-3.7 MBq contains approximately 1-3 µg Rituximab. Based on this knowledge, we administered either 1 or 3 µg of unlabeled Rituximab in 150 µL 0.9% sodium chloride (saline) solution intravenously to two separate groups of huCD20tg mice

alongside a group that received saline alone. After waiting 19 h for unlabeled Rituximab to circulate and bind CD20, we performed FACS of peripheral blood and spleens from these mice to quantify B cell numbers. We observed significant depletion of B cells in spleens of mice that had been treated with a single 3 μg dose of Rituximab compared with untreated mice (%CD19$^+$B220$^+$ lymphocytes: 31.94 ± 2.65 vs. 46.12 ± 2.04, p=0.002) and a trend toward reduction of B cells in blood (%CD19$^+$B220$^+$ lymphocytes: 43.20 ± 5.21 vs. 57.88 ± 1.29, p=0.09) (Fig. 2). There was no significant difference in %CD19$^+$B220$^+$ lymphocytes in spleens from mice treated with 1 μg compared to the saline group (44.72 ± 2.40 vs. 46.12 ± 2.04, p=0.66), however there was a slight trend towards B cell depletion in blood (1 μg-treated mice: 50.50 ± 4.37 vs. saline-treated mice: 57.88 ± 1.29, p=0.17). In accordance with these results, an upper limit of 1 μg Rituximab mass to be injected per mouse was set to ensure minimal effect on the population of cells we sought to image (~1.3-3.7 MBq, based on specific activity of a given batch). It should be noted that even at this very low mass amount utilized for PET imaging, subsequent B220 immunostaining (19 h after administration of tracer) showed that a portion of B cells exhibited a staining pattern and morphology indicative of some potential Rituximab induced cell damage/death in regions of the brain and spinal cord (Supplemental Fig. 3).

PET imaging results showed that ^{64}Cu-Rituximab-PET signal in lumbar spinal cord was significantly higher in huCD20tg EAE mice compared to controls, as early as 1h post-injection of radiotracer (lumbar: 5.44±0.37 vs. 3.33±0.20%ID/g, p<0.05) (Fig. 3A, 3B). Additionally, there was a strong trend toward higher uptake in the cervical/thoracic region of spinal cord (4.15±0.28 vs. 3.23±0.18%ID/g, p=0.057). Uptake in specific brain regions ranged between 1.74±0.11 and 2.93±0.15%ID/g for EAE mice compared to 1.25±0.08 and 2.24±0.11%ID/g for controls – p<0.05 for all regions except striatum and thalamus. Similar differences in CNS uptake for EAE and control mice were observed at both 4h and 19h post-injection of ^{64}Cu-Rituximab (Fig. 3C, 3D). Specificity of ^{64}Cu-Rituximab-PET signal for human CD20 was confirmed by imaging C57BL/6 mice with the same EAE score as huCD20tg EAE mice (i.e., 2.5-4.0). Results from these studies demonstrated significantly lower ^{64}Cu-Rituximab-PET signal in C57BL/6 EAE mice (devoid of human CD20) compared to huCD20tg EAE mice in cervical/thoracic (2.31±0.05 vs. 4.15±0.28%ID/g, p=0.0005) and lumbar spinal cord (2.24±0.12 vs. 5.44±0.37%ID/g, p<0.0001), as well as certain brain regions (i.e., cortex, hypothalamus, medulla, and pons, p<0.05) at 1 hour post-injection of tracer (Supplemental Fig. 4).

B220 immunostaining of CNS tissues from mice that underwent PET imaging verified that increased ^{64}Cu-Rituximab uptake in brain and spinal-cord

regions corresponded with elevated numbers of B220 positive cells (brain and meninges: naïve 0.14 ± 0.06 vs. EAE 4.42 ± 1.57, p=0.029; lumbar spinal cord: naïve 3.61 ± 0.28 vs. EAE 28.12 ± 14.55, p=0.114) (Fig. 3E).

Biodistribution results corroborated PET imaging data – revealing significantly elevated ^{64}Cu-Rituximab uptake in spinal cord of huCD20tg EAE mice (lumbar: 1.05±0.12 vs. 0.21±0.04%ID/g; thoracic/cervical: 0.69 ± 0.10 vs. 0.20 ± 0.04%ID/g, p<0.01) and a trend toward elevated ^{64}Cu-Rituximab binding in whole brain of EAE mice (0.23 ± 0.04 vs. 0.11 ± 0.02%ID/g, p=0.09) (Fig. 4A). The only significant difference in ^{64}Cu-Rituximab uptake in peripheral tissues was observed in spleen, whereby there was higher signal in EAE compared to age-matched control mice (21.70 ± 2.27 vs. 6.34 ± 0.87%ID/g, p<0.01) (Fig. 4A).

Digital autoradiography spinal cord results agreed with findings from *ex vivo* biodistrubtion and *in vivo* PET imaging. That is, there was significantly greater signal in EAE compared to control mice (mean pixel intensity in lumbar: 5360 ± 404.9 vs. 2332 ± 72.96, p<0.01; cervical/thoracic: 3160 ± 323.4 vs. 2001 ± 178.2, p<0.01) (Fig. 4B, 4C).

DISCUSSION

B cells play a critical role in MS, both in humans and mouse models. Meningeal inflammation, including the presence of B cell FLS, has been observed in early/relapsing MS patients, while B cell rich aggregates are associated with lesions reported in progressive disease (*3*). Unfortunately, these pathology studies are complicated by both the need for invasive biopsy (or can only be completed at postmortem) and the technical difficulty of maintaining the integrity of the meningeal compartment during tissue processing (*2*). In contrast, PET imaging offers the opportunity to noninvasively and longitudinally image molecular markers of disease. This current study demonstrates the promise of using ^{64}Cu-Rituximab to non-invasively visualize B cells in huCD20tg EAE mice.

The huCD20tg mouse model was uniquely suited for this work, as B cells in these mice have been engineered to express the human CD20 cell surface protein. While previous work has shown that human CD20 expression by B cells does not affect the onset or severity of autoimmune encephalitis in EAE mice, B220 immunostaining performed as part of the current work confirmed the formation of B cell FLS in the meninges and the presence of B cells in the brain and spinal cord. huCD20tg EAE mice thus recapitulated the gross pathology seen in traditional C57BL/6 models and provided a clinically relevant platform to assess the ability of ^{64}Cu-Rituximab to detect B cells in MS. Since the number of B cells in huCD20tg EAE mice and MS patients does not necessarily correlate

18

with disease severity (but can instead be used as an indicator of who will likely respond to anti-B cell therapies) we did not assess ^{64}Cu-Rituximab uptake in huCD20tg EAE mice of different disease scores.

Rituximab is an anti-human-CD20 monoclonal antibody that has shown promising therapeutic results in patients with arthritis and non-Hodgkin's lymphoma and has also been investigated for use in MS (*3*). Its high specificity and affinity for the B cell selective marker CD20, coupled with its preliminary success as a therapeutic in MS clinical trials, make Rituximab an ideal choice for a readily translatable PET tracer for imaging B cells in MS. Data from our *in vivo* PET imaging, *ex vivo* biodistribution, and autoradiography studies suggest ^{64}Cu-Rituximab is capable of imaging B cells in the spinal cord and brain of EAE mice. Histological analysis of CNS tissues from the same mice corroborated that the signal from ^{64}Cu-Rituximab corresponded well with regions of B cell infiltration. Specificity of ^{64}Cu-Rituximab for detecting human CD20-expressing B cells in huCD20tg EAE mice was confirmed by imaging C57BL/6 EAE mice (devoid of human CD20 target) – revealing a significantly diminished PET signal in spinal cord, cortex, hypothalamus, medulla, and pons.

Despite the promise of ^{64}Cu-Rituximab as an imaging agent, it has some disadvantages including brain availability and B cell depletion. Antibodies

generally have low brain uptake when the blood brain barrier is intact. In the current work this was a moot point due to the well-known blood brain barrier impairment in EAE mice (*15*). Since there is also blood brain barrier disruption in MS (*16*), it may feasible to image B cells with ^{64}Cu-Rituximab in MS patients, however this will need to be confirmed in future studies. Second, the high therapeutic potency of Rituximab, even at trace amounts of mass, is dose-limiting. The finding via FACS that Rituximab can induce significant B cell depletion in the spleen even at a low dose administration of 3 μg is important, as an ideal imaging agent should not perturb underlying biology one wishes to study. For this reason, we chose to utilize a dose < 1 μg for imaging. Although a mass of < 1 μg did not demonstrate significant B cell depletion in our studies, we cannot rule out minor effects on B cells. For example, we observed a trend towards intravascular depletion and some abnormalities in B cell appearance in tissue sections that may reflect a slight "therapeutic" injury to B cells in the mice imaged with ^{64}Cu-Rituximab. One consequence of these findings likely includes not being able to perform multiple imaging studies in the same mice without affecting underlying B cell biology, and thus another technique may be needed for therapy monitoring studies. Given these challenges, it is important to consider new protein engineering techniques being used to develop binders with altered pharmacologic properties. In the case of ^{64}Cu-Rituximab, which promotes Fc mediated depletion

by monocytes/macrophages, engineered variants could be designed to have an inert or absent Fc domain.

Further work should focus on investigating engineered protein variants and seeking to identify additional biomarkers that have potential to elucidate pathologically relevant from normal B cells in detrimental autoimmune diseases. For clinical studies, further optimization of specific activity/tracer-dose may be required to ensure no impact on B cells. It is possible however that mice with human CD20-expressing B cells could be more sensitive to low doses of Rituximab than what might occur in the clinical setting. As we move toward evaluating this tracer for clinical imaging of MS patients, we will assess the effect of varying tracer mass amounts of Rituximab on B cells in blood and we will adjust the dose if necessary.

CONCLUSION

Overall, the current work contains strong proof of concept data that ^{64}Cu-Rituximab is capable of imaging B cells in a murine model of MS. These data support further investigation of ^{64}Cu-Rituximab in preclinical models and translation as a possible clinical tool, for helping identify which MS patients are

most likely to respond to anti-B cell therapies and for monitoring real-time response.

Disclaimer

Sudeep Chandra is an employee of Novartis Institute of Biomedical Research.

REFERENCES

1. Krumbholz M, Derfuss T, Hohlfeld R, Meinl E. B cells and antibodies in multiple sclerosis pathogenesis and therapy. *Nat rev neurol*. 2012;8:613–23.

2. Serafini B, Rosicarelli B, Magliozzi R, Stigliano E, Aloisi F. Detection of ectopic B-cell follicles with germinal centers in the meninges of patients with secondary progressive multiple sclerosis. *Brain pathol*. 2004;14:164–174.

3. Castillo-Trivino T, Braithwaite D, Bacchetti P, Waubant E. Rituximab in Relapsing and Progressive Forms of Multiple Sclerosis: A Systematic Review. *PLoS one*. 2013;8.

4. Gasperi C, Stüve O, Hemmer B. B cell-directed therapies in multiple sclerosis. *Neurodegener dis manag*. 2016;6:37–47.

5. Lucchinetti C., Brück W., Parisi J., et al. Heterogeneity of multiple sclerosis lesions: Implications for the pathogenesis of demyelination. *Ann neurol*. 2000;47:707–717.

6. Monson NL, Cravens P, Hussain R, et al. Rituximab therapy reduces organ-specific T cell responses and ameliorates experimental autoimmune encephalomyelitis. *PLoS one*. 2011;6:1–6.

7.   Natarajan A, Gowrishankar G, Nielsen CH, et al. Positron emission tomography of 64Cu-DOTA-rituximab in a transgenic mouse model expressing human CD20 for clinical translation to image NHL. *Mol imaging biol*. 2012;14:608–616.

8.   Muylle K, Flamen P, Vugts DJ, et al. Tumour targeting and radiation dose of radioimmunotherapy with ^{90}Y-rituximab in CD20+ B-cell lymphoma as predicted by ^{89}Zr-rituximab immuno-PET: impact of preloading with unlabelled rituximab. *Eur j nucl med mol imaging*. 2015;42:1304–1314.

9.   Ilovich O, Natarajan A, Hori S, et al. Development and Validation Companion Diagnostic Agent for Antibody-Drug Conjugate Therapy to Target the CA6. *Radiology*. 2015;276:191–198.

10.   Rowlinson-Busza G. Determination of the immunoreactivity of Radiolabeled Monoclonal Antibodies. *Methods mol med*. 2000;40:351–61.

11.   James ML, Shen B, Zavaleta CL, et al. New positron emission tomography (PET) radioligand for imaging σ-1 receptors in living subjects. *J med chem*. 2012;55:8272–82.

12.   Haugen M, Frederiksen JL, Degn M. B cell follicle-like structures in multiple sclerosis-With focus on the role of B cell activating factor. *J neuroimmunol*. 2014;273:1–7.

13.   Uchida J. The Innate Mononuclear Phagocyte Network Depletes B

Lymphocytes through Fc Receptor-dependent Mechanisms during Anti-CD20 Antibody Immunotherapy. *J exp med*. 2004;199:1659–1669.

14. Reff ME, Carner K, Chambers KS, et al. Depletion of B cells in vivo by a chimeric mouse human monoclonal antibody to CD20. *Blood*. 1994;83:435–445.

15. Kipp M, van der Star B, Vogel DYS, et al. Experimental in vivo and in vitro models of multiple sclerosis: EAE and beyond. *Mult scler relat disord*. 2012;1:15–28.

16. Ortiz GG, Pacheco-Moisés FP, Macías-Islas MÁ, et al. Role of the blood-brain barrier in multiple sclerosis. *Arch med res*. 2014;45:687–97.
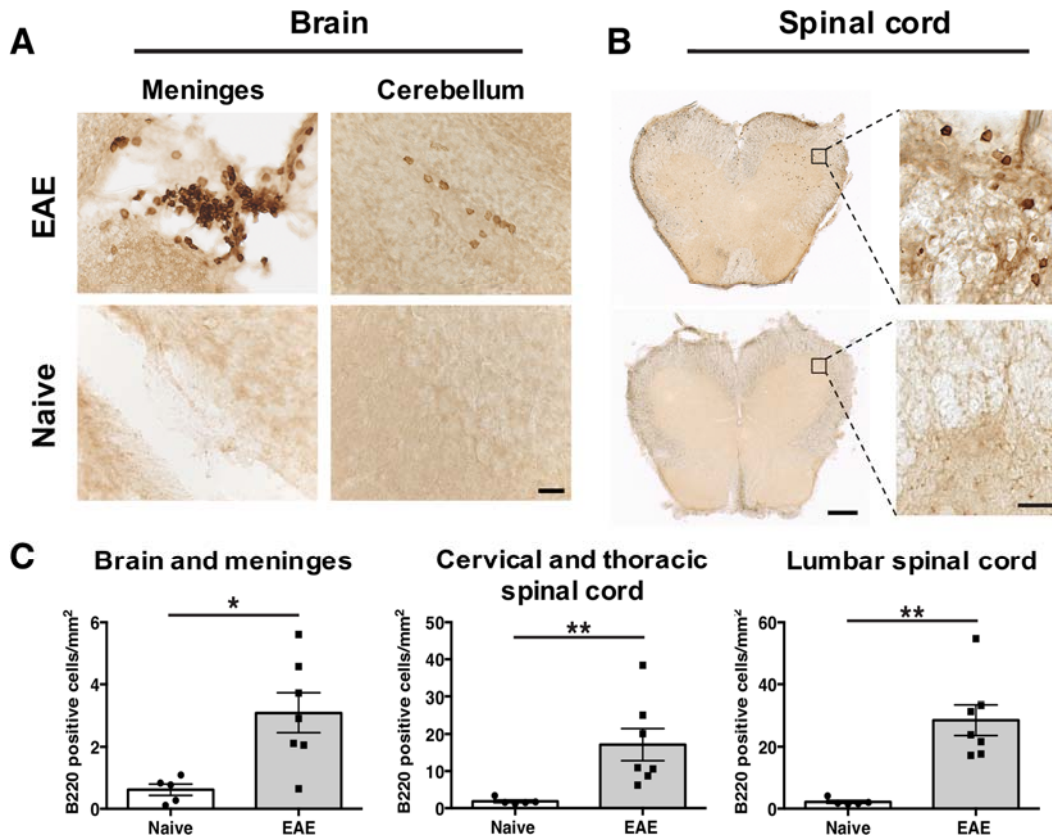
Fig. 1. Representative images of B220^{+} B cells in huCD20tg mouse (A) brain and (B) spinal cord. Scale bars: 25 μm in high-magnification and 500 μm in low-magnification images. (C) Quantitation of B220 positive cells per mm^2 in CNS tissues from EAE ($n = 7$) versus naive ($n = 5$) mice. *p <0.05, **p<0.01.
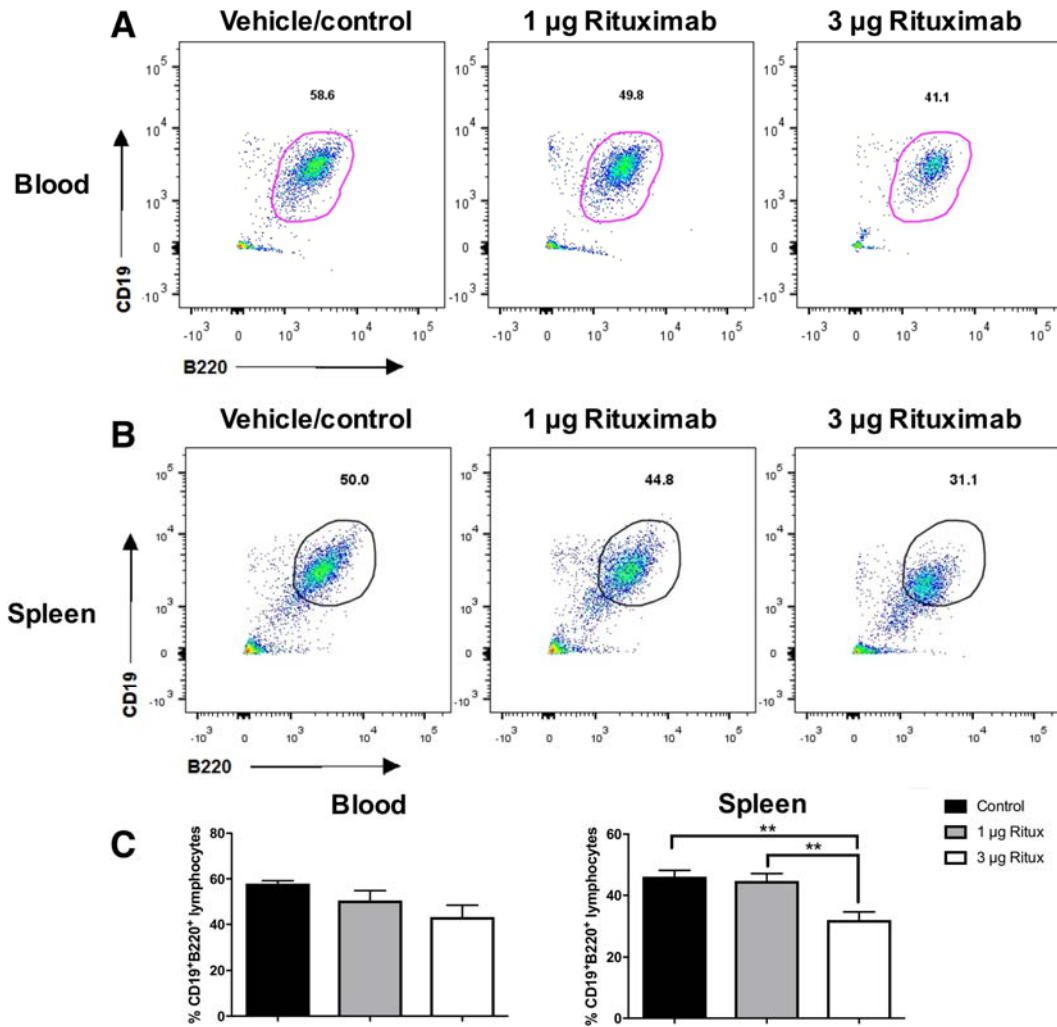
Fig. 2. FACS gating for (A) blood and (B) spleen. (C) Percentage of CD19$^+$B220$^+$ cells in blood and spleen from huCD20tg mice, 19 hours after single intravenous dose of Rituximab (1 μg or 3 μg) or saline. **p-value <0.01.
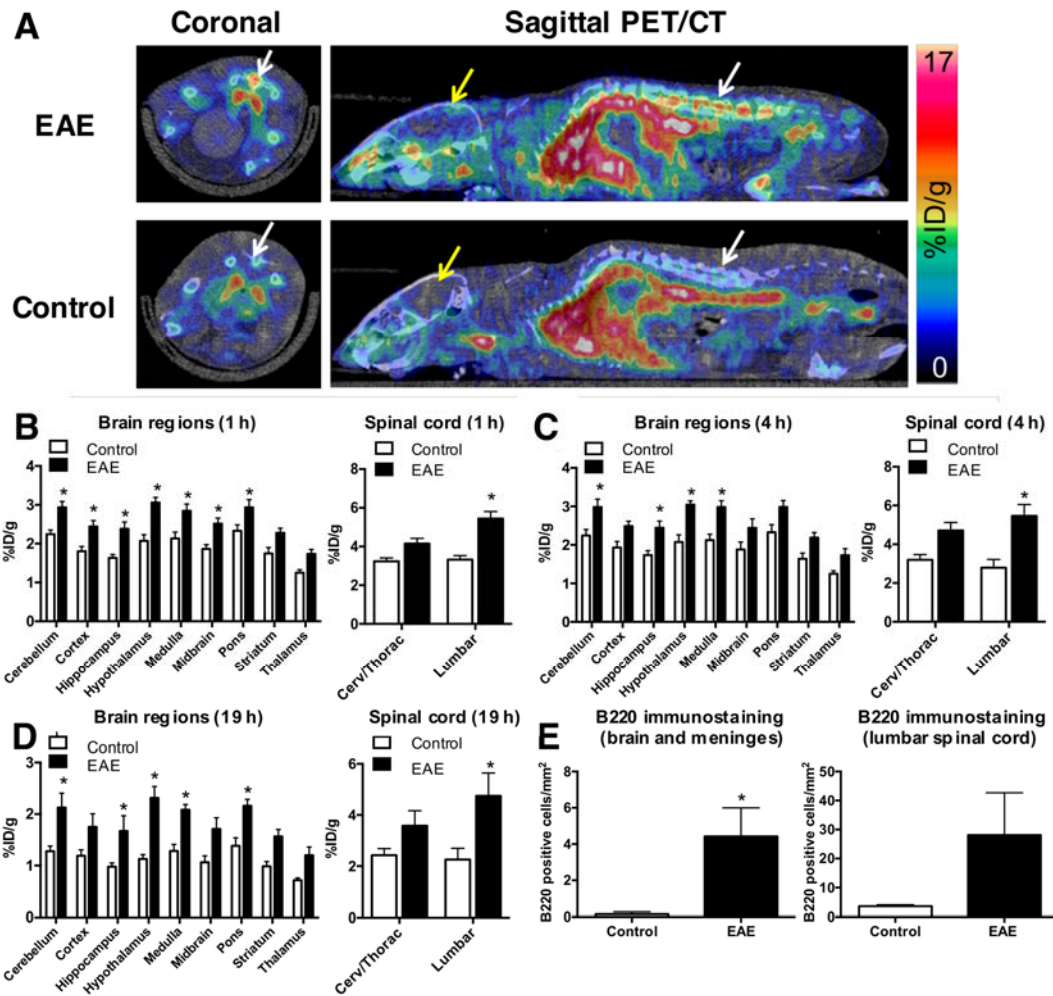
Fig. 3. (A) Representative PET/CT images 1 hour after ^{64}Cu-Rituximab injection. White and yellow arrows point to spinal cord and brain respectively. Graphs depict ^{64}Cu-Rituximab uptake in brain and spinal cord regions of EAE and control mice, quantified from PET images (B) 1 h, (C) 4 h, and (D) 19 h after tracer injection. (E) Quantitation of B220 positive cells per mm^2 in CNS tissues from EAE and control mice 19 hours after ^{64}Cu-Rituximab. *p <0.05, n = 4 per group.
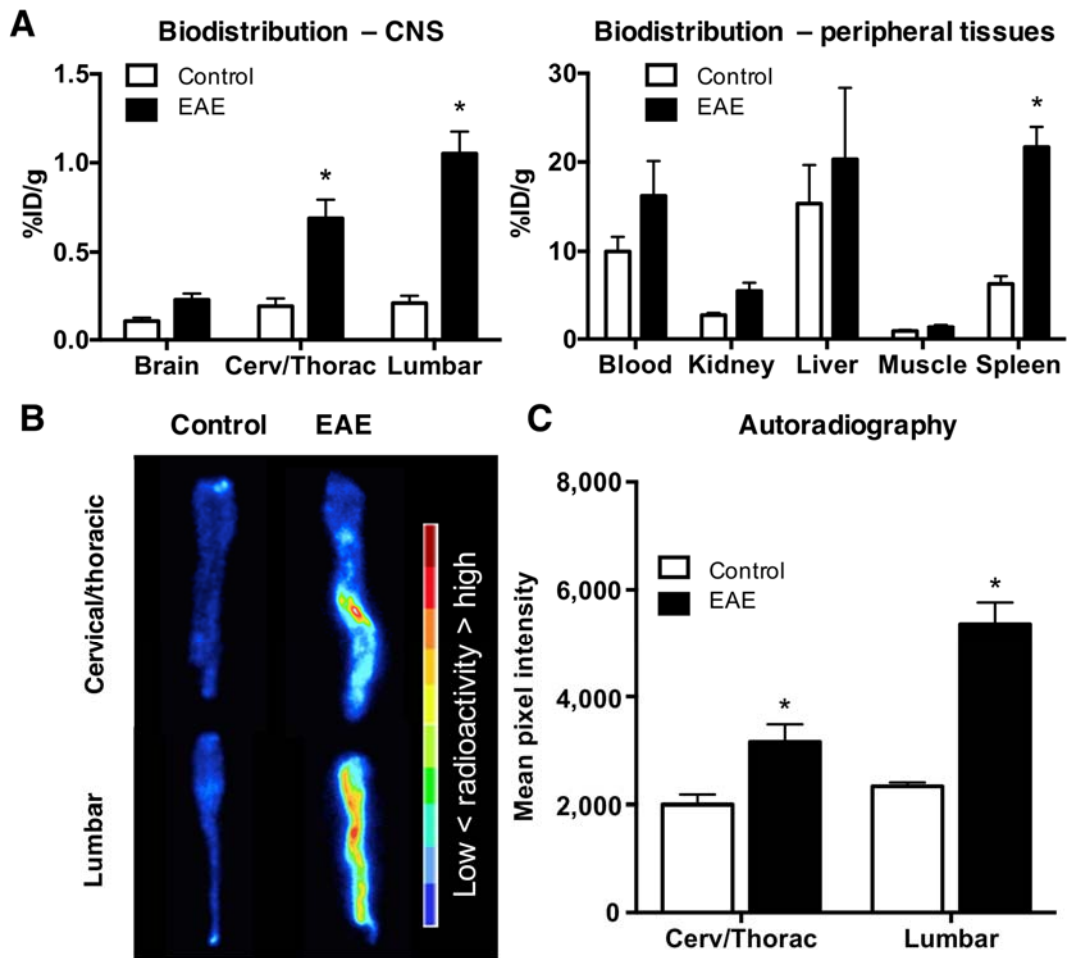
28

Fig. 4. (A) ^{64}Cu-Rituximab biodistribution in CNS and peripheral tissues, 24 hours post-injection, $n = 5$ per group. (B) Images and (C) quantitation of spinal cord autoradiography from EAE and control mice, $n = 3$ per group. *p-value <0.05.

Supplemental:

Imaging B cells in a mouse model of multiple sclerosis using ^{64}Cu-Rituximab-PET

Michelle L. James[1,2], Aileen Hoehne[1], Aaron Mayer[1], Kendra Lechtenberg[2], Monica Moreno[2], Gayatri Gowrishankar[1], Ohad Ilovich[1], Arutselvan Natarajan[1], Emily M. Johnson[1,2], Joujou Nguyen[1], Lisa Quach[2], May Han[2], Marion Buckwalter[2], Sudeep Chandra[3], Sanjiv S. Gambhir[1]*.

Affiliations:

[1]*Department of Radiology, Stanford University, CA, 943065, USA*

[2]*Department of Neurology and Neurological Sciences, Stanford University, CA, 943065, USA*

[3]*Clinical and Translational Imaging, Novartis Institute of Biomedical Research, Cambridge, USA.*


*Corresponding Author: Sanjiv S. Gambhir, 318 Campus Dr, E150, Stanford, CA 94305, USA. V: (650)725-6175; F: (650)723-8649 (sgambhir@stanford.edu).

First Author: Michelle L. James (Instructor), 3165 Porter Drive, Stanford, CA 94304. V: (650)721-3324; F: (650)724-4948 (mljames@stanford.edu).
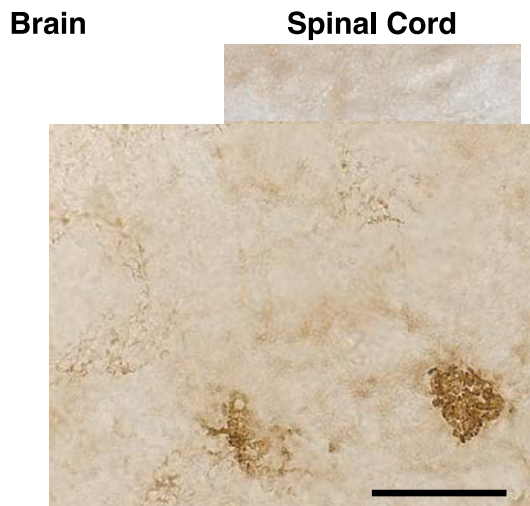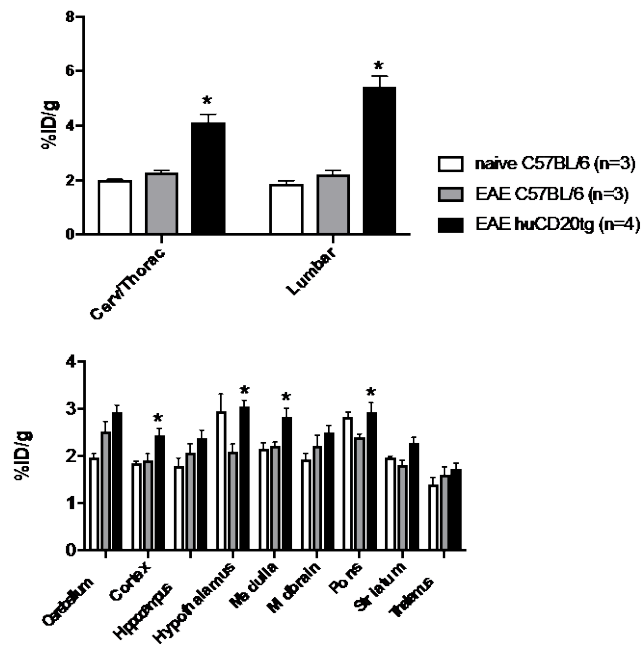
Figures
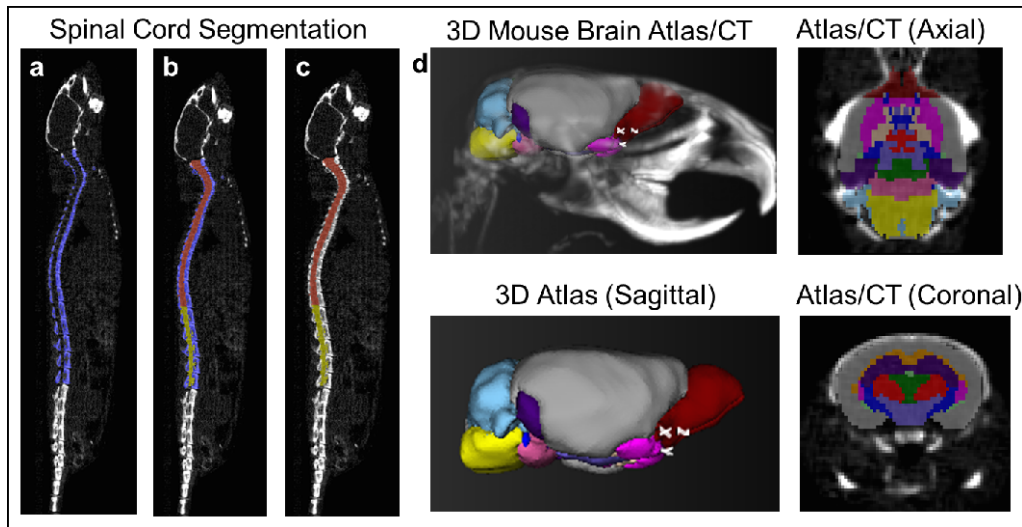
Supplemental Figure 1. (a) Using Vivoquant, the spine (blue) was segmented out with Otsu Thresholding. (b) The spine ROI was made immutable, and the thoracic/cervical (orange) and lumbar (yellow) spinal cord ROI's were drawn in using a 3D drawing tool. The lumbar began at the first vertebrate above the pelvis, and the thoracic started after the 5th vertebrate from the bottom. (c) The spine was then removed, and the data from the lumbar and thoracic/cervical spinal cord were obtained. (d) The brain ROI contained the following regions using Whole Brain Atlas within Vivoquant: medulla (yellow), cerebellum (light blue), midbrain (dark green), pons (light pink), cortex (grey), thalamus (red), hypothalamus (light purple), hippocampus (dark purple), striatum (magenta), pallidum (peach), olfactory bulbs (maroon), corpus callosum (orange), white matter (dark blue), ventricles (light green). After fitting to the CT, the activity levels (nCi/cc) in each region were obtained.
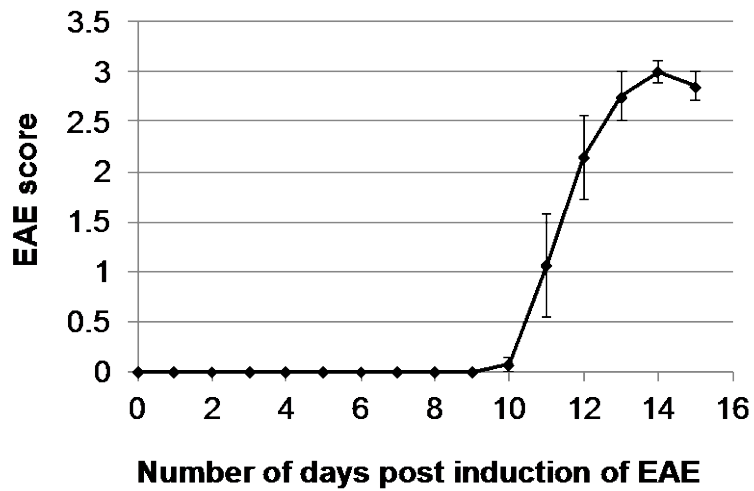
Supplemental Figure 2. EAE Induction in HuCD20 Mice. Average EAE score on each day after induction of EAE. n=20 female huCD20tg mice; aged >10 weeks.

Supplemental Figure 3. Representative 63X magnification images of B220 immunostained (A) intact and (B) fragments of B cells in brain and spinal cord 19-20 hours after single PET tracer dose (1 µg) of ^{64}Cu-Rituximab. Scale bar = um.

Supplemental Figure 4. Elevated ^{64}Cu-Rituximab-PET signal in spinal cord and certain brain regions is specific for human CD20-expressing B cells. Graphs depict uptake (i.e., % injected dose per gram, %ID/g) of ^{64}Cu-Rituximab in brain and spinal cord regions of naïve C57BL/6 mice, EAE C57BL/6 mice, and huCD20tg EAE mice quantified from PET images 1h after tracer injection. Mean +/- SEM *p-value <0.05, two-way ANOVA.